Visual receptive field properties of cells in the optic tectum of the archer fish

Mor Ben-Tov, Ivgeny Kopilevich, Opher Donchin, Ohad Ben-Shahar, Chen Giladi and Ronen Segev

J Neurophysiol 110:748-759, 2013. First published 8 May 2013;
doi: 10.1152/jn.00094.2013

Journal of Neurophysiology publishes original articles on the function of the nervous system. It is published 24 times a year (twice monthly) by the American Physiological Society, 9650 Rockville Pike, Bethesda MD 20814-3991. ESSN: 1522-1598. Visit our website at http://www.the-aps.org/.

J Neurophysiol 110: 748–759, 2013.
First published May 8, 2013; doi:10.1152/jn.00094.2013.

Visual receptive field properties of cells in the optic tectum of the archer fish

Mor Ben-Tov,[1,2] Ivgeny Kopilevich,[2,3] Opher Donchin,[2,3,4] Ohad Ben-Shahar,[2,5] Chen Giladi,[6] and Ronen Segev[1,2]

[1]*Department of Life Sciences, Ben-Gurion University of the Negev, Be'er-Sheva, Israel;* [2]*Zlotowski Center for Neuroscience, Ben-Gurion University of the Negev, Be'er-Sheva, Israel;* [3]*Department of Biomedical Engineering, Ben-Gurion University of the Negev, Be'er-Sheva, Israel;* [4]*Department of Neuroscience, Erasmus University Medical Center, Rotterdam, The Netherlands;* [5]*Department of Computer Science, Ben-Gurion University of the Negev, Be'er-Sheva, Israel; and* [6]*Department of Physics, Ben-Gurion University of the Negev, Be'er-Sheva, Israel*

Submitted 5 February 2013; accepted in final form 7 May 2013

Ben-Tov M, Kopilevich I, Donchin O, Ben-Shahar O, Giladi C, Segev R. Visual receptive field properties of cells in the optic tectum of the archer fish. *J Neurophysiol* 110: 748–759, 2013. First published May 8, 2013; doi:10.1152/jn.00094.2013.—The archer fish is well known for its extreme visual behavior in shooting water jets at prey hanging on vegetation above water. This fish is a promising model in the study of visual system function because it can be trained to respond to artificial targets and thus to provide valuable psychophysical data. Although much behavioral data have indeed been collected over the past two decades, little is known about the functional organization of the main visual area supporting this visual behavior, namely, the fish optic tectum. In this article we focus on a fundamental aspect of this functional organization and provide a detailed analysis of receptive field properties of cells in the archer fish optic tectum. Using extracellular measurements to record activities of single cells, we first measure their retinotectal mapping. We then determine their receptive field properties such as size, selectivity for stimulus direction and orientation, tuning for spatial frequency, and tuning for temporal frequency. Finally, on the basis of all these measurements, we demonstrate that optic tectum cells can be classified into three categories: orientation-tuned cells, direction-tuned cells, and direction-agnostic cells. Our results provide an essential basis for future investigations of information processing in the archer fish visual system.

archer fish; optic tectum; early visual processing; retinotectal mapping; orientation and direction selectivity

IN RECENT YEARS, THE ARCHER FISH has proved to be a very productive model in the study of many aspects of visual behavior, from retinal encoding (Tsvilling et al. 2012; Vasserman et al. 2010), eye movements (Ben-Simon et al. 2009), animal competition (Schuster 2011), and visual acuity (Ben-Simon et al. 2012a; Temple et al. 2010, 2013) to tracking of moving targets (Ben-Simon et al. 2012b; Schlegel and Schuster 2008; Schuster et al. 2006; Timmermans 2000, 2001) and visual search (Mokeichev et al. 2010). The productivity of the model can be explained, in part, by the ability of the archer fish to overtly report its visual decisions by employing a squirt of water from its mouth aimed at selected targets. The archer fish can be trained to shoot at a variety of artificial targets from small food pellets to printed targets on paper and even targets presented on computer monitors. Thus complex experiments of recognition and decision making can be conducted with careful experimental settings to explore various aspects of visual information processing in a psychophysically rigorous manner.

Address for reprint requests and other correspondence: R. Segev, Dept. of Life Sciences, Ben-Gurion Univ. of the Negev, Be'er-Sheva 84105, Israel (e-mail: ronensgv@bgu.ac.il).

In addition to the advantages described above, the archer fish is an interesting animal to study as a fish with a semiterrestrial visual environment. Put differently, it is an animal that, like most mammals, processes a visual landscape above water level, while as a fish, it does so with a brain whose structure is very different from that of mammals. Thus studies of the visual processing in the archer fish can lead to broader perspective on the functional properties of visual systems that have to cope with such environment.

The central unit of the fish visual information processing is the optic tectum. The information from each eye travels directly to the tectal lobe on the opposite side of the brain, where information processing work flow is believed to occur (Kinoshita and Ito 2006; Kinoshita et al. 2002; Vanegas and Ito 1983). Information processing in the mammalian visual cortex appears to progress hierarchically, where the visual stream ascends from one cortical region to another with progressive representation and processing of visual information. The optic tectum of fish, however, appears to be much more uniform across the tectum surface in terms of functional units (Nevin et al. 2010); i.e., the cells in the optic tectum are diverse in their response to different features of the visual stimuli, and they are not arranged in columnar organization. Furthermore, next to visual signals from the retina, input from other sensory modalities such as auditory, lateral line, and somatosensory are also mapped topographically over the tectum (Bodznick 1990; Catania et al. 2010; Knudsen 1982). Anatomically, it was found in other teleosts that the most important distinction is between the superficial layers, which are mainly visual, and the deep layers, which are multimodal and motor (Bastian 1982; Bodznick 1990). Focusing on vision, we have therefore selected the superficial layers of the archer fish optic tectum as our target of research.

Studies have described the retinotectal maps in fish by recording from the superficial tectum using single electrodes (Jacobson and Gaze 1964; Schwassmann and Kruger 1965). These studies showed that there is correspondence between dorsal and rostral points within the visual field of the eye and points in the contralateral tectum. In addition, research was devoted to find the size of the receptive fields. It was found that the smallest size of the receptive field was 7.7° and 1.8° for zebra fish and goldfish, respectively (Damjanović et al. 2009b; Sajovic and Levinthal 1982). Knowledge about spatial mapping between the primary visual area of the fish and the visual field and the sizes of the receptive fields can provide the opportunity for further investigation of spatial discrimination and visual acuity.

Seeking to study the overall functional organization of the optic tectum of archer fish, the specific purpose of our present work is twofold: *1*) to reveal the retinotectal mapping of the archer fish optic tectum, and *2*) to describe the functional properties of the receptive field of optic tectum cells. Our results will thus provide a foundation for future studies of visual processing in the archer fish and of the mapping between its visual behavior and neural visual processing.

MATERIAL AND METHODS

Animals

All experiments with fish were approved by the Ben-Gurion University of the Negev Institutional Animal Care and Use Committee and were in accordance with government regulations of the State of Israel. Twenty-eight archer fish (*Toxotes chatareus*; Fig. 1*A*), 6–13 cm in length, 10–15 g body weight, were used in this study. The fish were normally kept in a water tank 50 × 70 × 30 cm in size (~100 liters) filled with brackish water (2–2.5 g of red sea salt mix for 1 liter of water) at 26–28°C. The room was illuminated with artificial light with a 16:8-h day-night cycle.

Surgery

Fish were anesthetized with MS-222 (100 mg per liter of tank water; A-5040, Sigma). The pH level was adjusted to compensate for MS-222 acidity. After the fish lost its buoyancy balance and flipped onto its back, it was restrained in a special device and its gills were watered continuously with tank water containing MS-222. The watering of the gills was essential due to a possible respiratory failure

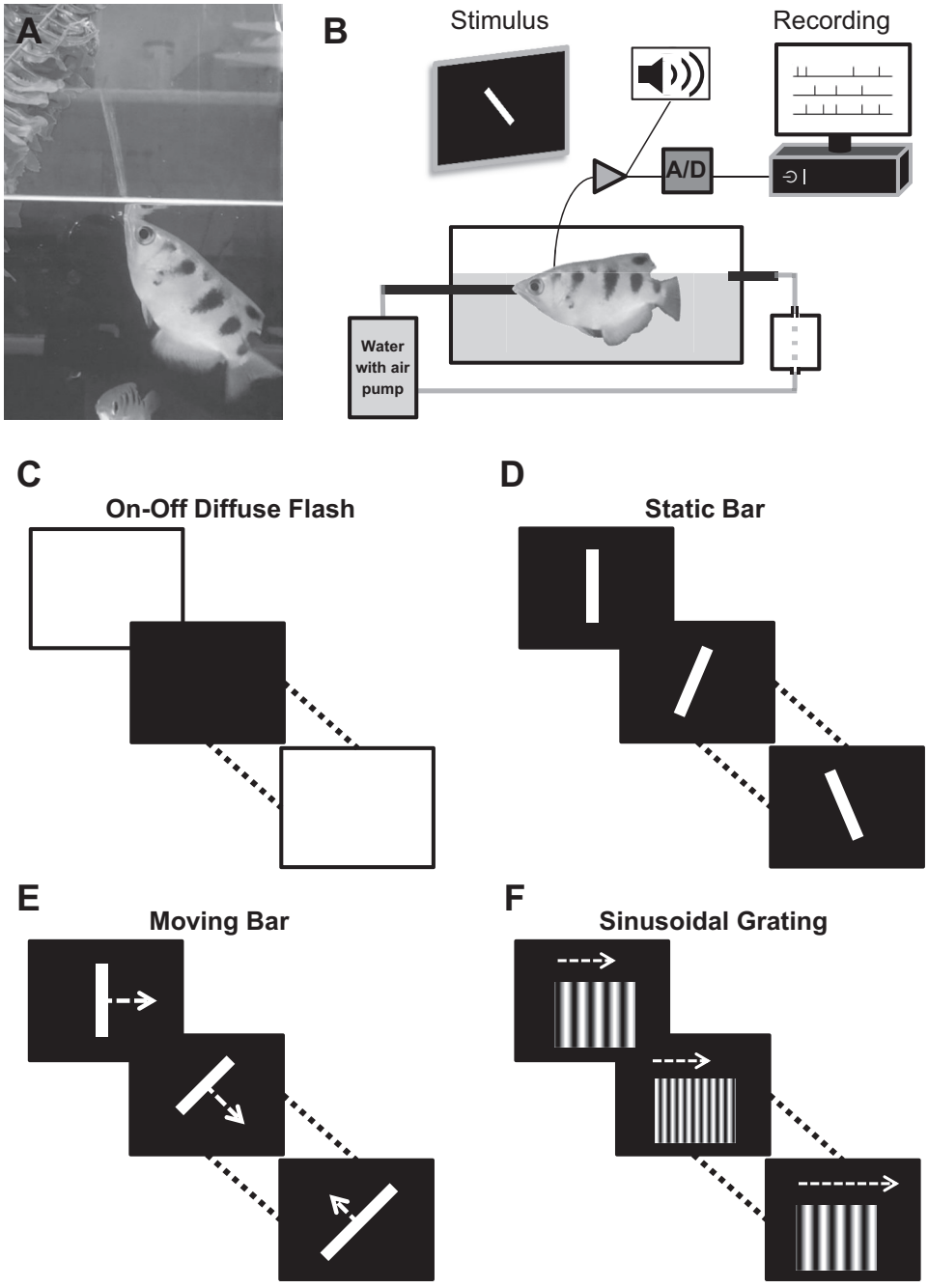

Fig. 1. The archer fish and the experimental setup. *A*: an archer fish shoots at an insect above water level. *B*: a schematic view of the experimental setup, which consists of a monitor to present the stimuli, a recording setup of 1 extracellular electrode, and a life support system for the fish. The fish's gills were continuously watered through a tube inserted into its mouth. The water reservoir is equipped with air pump that helps insufflate air in the water tank so that oxygen is available to the fish. A stream breaker device is used to prevent an electrical current from passing through the water molecules. *C–F*: the 4 types of visual stimuli used in the experiment. *C*: on-off diffuse flash, a repeating loop consisting of 1 s of white screen followed by 1 s of black screen. *D*: static bar, a stationary bar in 8 different orientations (orientations varied by 22.5°). *E*: moving bar, a bar moving in 8 different directions (directions varied by 45°). The direction of motion was orthogonal to the bar's orientation. *F*: sinusoidal gratings, drifting in different spatial and temporal frequencies. Spatial frequency varied between 0.03 and 0.7 cycles/deg (6 logarithmic steps), and temporal frequency varied between 1.5 and 9 cycles/s (6 linear steps).

caused by exposure to MS-222. An incision was made over the optic tectum, the skin and fatty tissue were removed, and lidocaine (L-7757, Sigma) was applied to the boundaries of the incision. At this point we injected the fish with 5–15 μl of the nondepolarizing muscle relaxant gallamine triethiodide (17 g/l; G 8134, Sigma) to its spine, toward its tail, to prevent muscle movement during the experiment. Specifically, we confirmed that the eye movements of the fish were eliminated, and only then did we continue with the rest of the procedure. A dental drill (Fine Science Tools micro drill, no. 097883, with a 2.7-mm tip diameter; stainless steel trephines, no. 18004-27) was then used to open the skull and meninges over the optic tectum. A silver wire (76.2-μm diameter, tip coated with silver chloride) was placed in the cerebrospinal fluid near the optic tectum to use as a reference electrode. The tectum was then covered with a thin layer of Vaseline to prevent its dehydration.

In Vivo Electrophysiology

The fish and the restraining device were placed together in a smaller water tank (length 25 cm, width 6 cm, height 6 cm) filled with brackish water (red sea salt, 2–2.5 g/l) up to 0.5 cm above eye level (no MS-222 at this stage; see Fig. 1*B*). The fish's gills were continuously watered through a tube inserted into its mouth to compensate for possible respiratory degradation. The fish was placed so that its right eye was 0.3 cm from the glass wall (parallel to the sagittal plane of the fish) in the center of the tank. This glass wall was higher than the other walls (12-cm height) and thus allowed the fish a wide visual field (about 110° in both the vertical and horizontal axes). Using a single electrode (tungsten, glass coated, 250-μm diameter, 2-MΩ impedance, 60-mm length; no. 366-060620-11, Alpha-Omega, Nazareth, Israel) mounted on a calibrated manipulator (Narishige, Tokyo, Japan), recordings were made from the superficial layers (up to 500 μm deep) of the optic tectum. The signal obtained was magnified ($\times 10^4$) and filtered (band-pass box filter, 300 Hz–10 kHz range) by an amplifier (DAM 50, WPI) and then transmitted through two parallel channels: *1*) the signal was sampled and recorded to a computer at 20 kHz, and *2*) the signal went through an analog notch filter (Hum Bug, Quest Scientific), removing 50 Hz, and then to an audio monitor (AM9, Grass Instruments) and an oscilloscope (TDS 210, Tektronix). In this way the neural response could be both heard and seen in real time during the experiment. The average duration of a typical recording session was ~5 h, and we were able to hold single units up to 30–40 min.

Spike Sorting

Spike sorting was done off line using an in-house Matlab program. First, the signal was filtered with a band-pass filter with additional noise reduction at 50-Hz frequency. Potential spikes were detected in events where the filtered signal crossed a threshold of 4.5 times the standard deviation of the signal. The peak in every segment was determined, and 1.5 ms of signal was kept before and after the peak. Using a graphical user interface, we manually removed events that did not have the shape of a spike. We then clustered the spikes into one or more groups based on spike amplitude and width.

Estimation of the Location of the Receptive Field

We stimulated the visual system using a hand-held flashlight to determine whether each single cell could produce a high-quality neural response. In well-isolated cells with a high-quality neural response, the stimulating computer screen was positioned 20 cm from the animal's eye. To estimate the location of the cell's receptive field, a white bar was moved interactively by the experimenter across the screen in different orientations and moving directions to detect the limits of the receptive field. The bar was moved across the screen until a strong reaction was heard; this point was marked as one of the edges of the receptive field. In a similar way, the bar was moved in different directions to determine the borders of the receptive field. This method enables us to mark the receptive field boundary fast enough that mapping of many cells from each animal was possible. The error in determining the exact location of the edges is ~1.5°.

Visual Stimuli and Data Analysis

Four types of stimuli were presented on the screen, and they are demonstrated in Fig. 1, *C–F*. All stimuli were generated using either the Psychophysics toolbox in Matlab or directly in C++.

ON-OFF stimulus. The ON-OFF stimulus consisted of 1 s of white screen followed by 1 s of black screen (light intensity values of 2.66 and 0.41 μW/cm^2, respectively) in 20–30 repeating loops (Fig. 1*C*). For each condition, we calculated the response as the mean number of spikes in a time window of 50 ms around the peak response time. After obtaining these responses, we computed the response ratio (R) as follows:

$$R = \frac{R_{ON} - R_{OFF}}{R_{ON} + R_{OFF}},$$

where R_{ON} is the response to the onset of the flash and R_{OFF} is the response to the offset of the flash.

Stationary bar. The stimulus consisted of a bar (white over black background) in eight different orientations (orientations step 22.5°; see Fig. 1*D*). The length and width of the bar were adjusted to match the receptive field size, as estimated by the initial stimulation procedure (see above). Each bar presentation was followed by 0.5 s of black screen, to avoid any adaptation effects, in 7–12 repeating loops. For each orientation, we calculated the response as the average firing rate in a time window of 200 ms around the peak response time. To determine whether the cell is orientation tuned or not, we calculated the orientation index as follows:

$$\text{Orientation Index} = \frac{R_p - R_o}{R_p + R_o},$$

where R_p is the response rate at the preferred orientation and R_o is the response rate at the orthogonal orientation. According to previous studies (Baron et al. 2007; Wang et al. 2010), we used the value of 0.5 to distinguish between two cell classes: orientation-tuned cells and orientation-agnostic cells. Cells with orientation index $\geq$0.5 were considered orientation-tuned cells. We then fitted parametric curves to responses as a function of the orientation of the bar, to determine the width of the orientation tuning. The fit was based on the probability density function of the von Mises distribution (Fisher 1995) as described in *Eq. 1*:

$$M(x) = \frac{p \cdot e^{\kappa \cos(x-\mu)}}{2\pi I_0(\kappa)}, \quad (1)$$

where $I_0(x)$ is the modified Bessel function of order 0 and the fitted parameters are p, peak response; μ, center orientation at the peak; and κ, concentration factor.

We explored the parameter κ to find the orientation tuning width. The advantage in fitting a von Mises distribution to this kind of data is that it enables us not only to find the preferred orientation, but also to facilitate the extraction of data such as the tuning width.

Moving bar. A circle 120% of the receptive field size was drawn around the estimated receptive field location, and a bar, with length and width adjusted to match the receptive field size, was moved from one side of the circle to the opposite side (1 cycle per 1.5 s, followed by 0.5 s of black screen, to avoid any adaptation effects, in 7–12 repeating loops) with direction of motion orthogonal to the bar's orientation (8 different directions; see Fig. 1*E*). For each direction, we calculated the response as the mean number of spikes in a time window of 200 ms around the peak response time. To determine

whether the cell is direction tuned or not, we calculated the direction index as follows:

$$\text{Direction Index} = \frac{R_p - R_o}{R_p + R_o},$$

where R_p is the response rate at the preferred direction and R_o is the response rate at the opposite direction. Cells with direction index ≥ 0.5 were considered direction-tuned cells. For cells with direction index <0.5, we calculated the orientation index (as described above). Cells with orientation index ≥ 0.5 were considered orientation-tuned cells. We then fitted parametric curves to responses as a function of the direction of the bar to the cells with direction index ≥ 0.5, to determine the width of the direction tuning. The fit was based on a von Mises functions as described in *Eq. 1*.

For comparison, and for ensuring our results are robust, we also fitted the response of the cell to the different directions with a second-order harmonic function (HF) as suggested by Maximov et al. (2005):

$$HF(x) = a_0 + a_1 \cos(x - \mu_1) + a_2 \cos(2x - 2\mu_2), \qquad (2)$$

where a_i are the amplitude and μ_i are the phases of the different harmonics. The amplitudes of the harmonics (a_0, a_1, and a_2) were used to classify the cells into three different groups: direction-tuned, orientation-tuned, and direction-agnostic cells. Specifically, cells were classified as direction-tuned if their first harmonic had distinct relative amplitude, i.e., $a_1 > a_2$ and $a_1 > 0.5a_0$, as orientation-tuned ones if their second harmonic had distinct relative amplitude, i.e., $a_2 > a_1$ and $a_2 > 0.5a_0$, and as direction-agnostic ones if the relative amplitudes of both their first and second harmonics were small (Maximov et al. 2005).

Sinusoidal gratings. The stimulus consisted of drifting sinusoidal gratings (maximum and minimum light intensity values of 2.66 and 0.41 $\mu W/cm^2$, respectively) in different spatial and temporal frequencies (Fig. 1*F*). Each presentation of a grating appeared for 1.5 s, followed by 0.5 s of black screen, to avoid any adaptation effects, in 7–12 repeating loops. The direction of the grating was chosen to be the preferred direction obtained from the moving bar stimulus. Spatial frequency varied between 0.03 and 0.7 cycles/deg (6 logarithmic steps), and temporal frequency varied between 1.5 and 9 cycles/s (6 linear steps), resulting in a total of 36 grating conditions. Firing rates for each grating were obtained by averaging the number of spikes over the 1.5-s stimulus duration across all trials and subtracting the first 50 ms, to avoid the onset response. Collecting these responses for all stimulus conditions, we then determined the preferred spatial and temporal frequency combination for each cell. Finally, we evaluated the spatial frequency tuning at the preferred temporal frequency and the temporal frequency tuning at the preferred spatial frequency by fitting them with a Gaussian function.

Retinotectal Mapping of the Optic Tectum

To determine the gross mapping between the visual field to the optic tectum surface, we first took a photo of the optic tectum and aligned it to a grid consisting of small regions along the anterior-posterior and the medial-lateral axes. This procedure divided the optic tectum surface to small regions of interest (Fig. 2*A*). Once a well-isolated cell with a high-quality neural response was found, we marked the location of the penetration to the optic tectum on the photo we previously took. The accuracy of the determining the exact penetration point was ~0.4 mm. At the end, we grouped single units to those regions by their tectal location. For each unit, we estimated the receptive field dimension and location as described in above. We then assigned an average receptive field location and dimension for each grid region by averaging those properties of all cells that corresponded to that region. This procedure was done in different animals and allowed us to combine data from different experiments.

Estimation of Confidence Intervals on Cell Type Ratio in the Population

For each cell type ratio, we determined the 95% confidence intervals using the Clopper-Pearson method. In addition, we estimated the confidence interval of the event that there is an additional cell group we did not observe in the data set.

RESULTS

We measured the receptive field location and functional properties of cells in the optic tectum of the archer fish using extracellular electrodes. The fish was immobilized during experiments, and respiration was reduced by perfusing the gills. Overall, we measured from a total of 166 cells in 28 different animals in different stimulus conditions.

Retinotectal Map of Archer Fish Optic Tectum

To reveal the retinotectal mapping of receptive fields of cells in the optic tectum, we mapped the location of 35 cells in 5 different animals by using an interactively moving bar in different orientations. For each location on the optic tectum surface (see MATERIALS AND METHODS), we found several cells from different animals and measured the receptive field location and dimensions. The average location and dimension of each location on the optic tectum surface were then calculated to reveal the map between the specific place in the optic tectum and the location in the visual field (Fig. 2, *A* and *B*).

We found that the dorsal visual field projects to the lateral part of the optic tectum and the ventral visual field projects to the medial part of the optic tectum. The visual field in the nasal direction projects to the rostral part and visual field in the temporal direction projects to the caudal part of the tectum (Fig. 2, *A* and *B*).

In addition, we found that the receptive fields can be divided into two groups according to their location, size, and shape. The first group consists of cells with receptive fields in front of the fish's eye in the dorsal-ventral plane, i.e., at the same height as the fish eye. The second group consists of cells with receptive fields located more dorsally (Fig. 2*B*).

Exploring the shape of the receptive fields, we found that the majority of receptive fields that were located in front of the fish's eye in the dorsal-ventral plane were elongated in their vertical dimension (Fig. 2*C*, red, yellow, and green circles). In cells with receptive fields located more dorsally, the receptive fields were slightly more elongated in their horizontal dimension than in their vertical dimension (Fig. 2*C*, blue and cyan circles). A closer examination of the width and height of the receptive fields shows that the receptive fields of cells with receptive fields located in front of the fish's eye in the dorsal-ventral plane are significantly narrower and longer than receptive fields of cells with receptive fields located more dorsally, which were wider and shorter.

We determined the size of the receptive field as the geometrical mean of its two edges (Fig. 2*D*). We found that there was a significant difference in the size distribution of the two groups (Kolmogorov-Smirnov test, $P < 0.001$). Specifically, small receptive fields (range: 3.12°–9.48°, mean: 5.32°) were located above the temporal-nasal line. Large receptive fields of cells (range: 5.45°–17.69°, mean: 10.14°) were located in front of the fish eye.

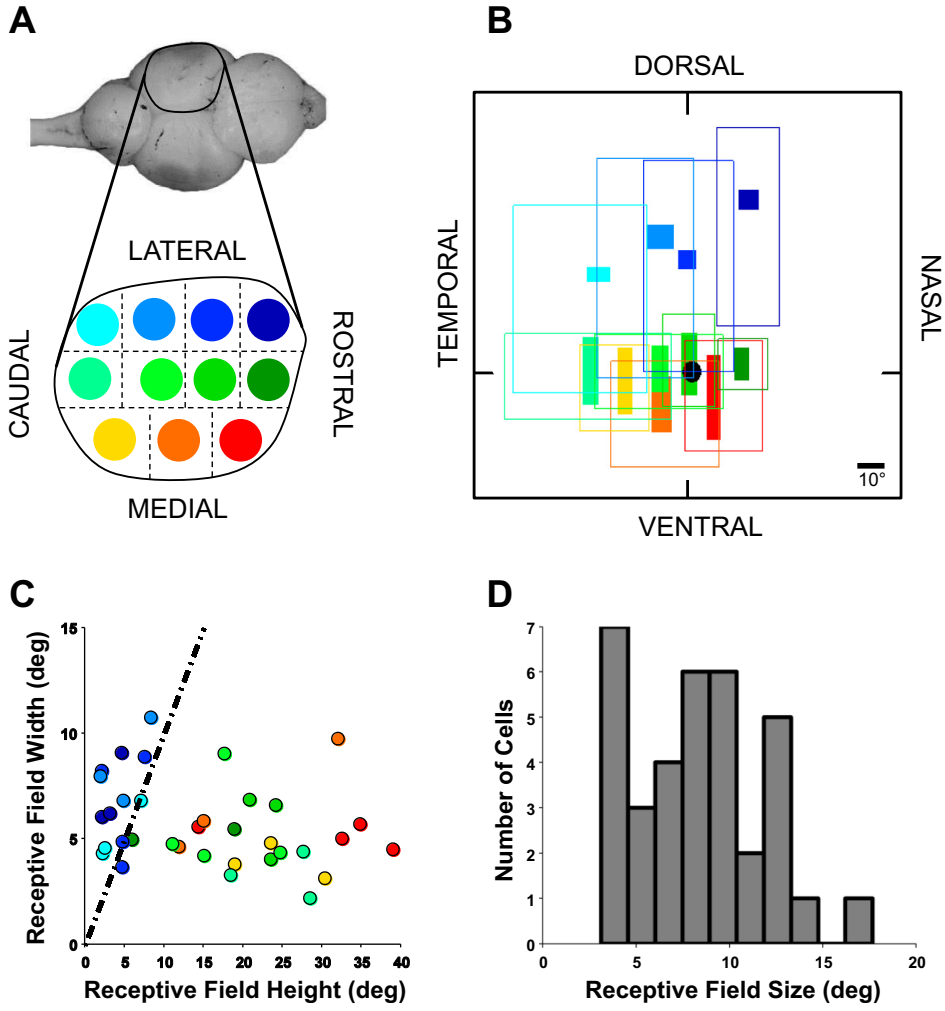

Fig. 2. Space and size organization of receptive fields in the archer fish optic tectum. *A*: a photo of the archer fish brain with the left optic tectum delineated (*top*) and the electrode positions on the left optic tectum (*bottom*). *B*: topographical arrangement of receptive fields in the right visual field of the archer fish. The black circle represents the fish eye. Each color corresponds to the electrode position shown in *A*. Solid rectangles represent the average receptive field location and dimension, and contour rectangles represent the area into which all the receptive fields belonging to the same grid fall. *C*: width of a receptive field as a function of its height. Each color corresponds to the electrode position shown in *A*. *D*: distribution of receptive field size.

In addition, we examined the area in which all the receptive fields belonging to the same grid fall (Fig. 2*B*, contour rectangles). We found that there is no significant difference in the widths of the circumscribed receptive field areas (permutation test, $P > 0.05$). However, there is a significant difference between the two groups in the variability in the dorsal-ventral axis (permutation test, $P < 0.01$). The height of the circumscribed area of the receptive fields closer to the fish eye is smaller than the height of the circumscribed area of the receptive fields located more dorsally.

Archer Fish Optic Tectum Cells Respond to an ON/OFF Stimulus

We tested the response of the cells to the onset and offset of a light by presenting a full-field flash stimulus. We recorded a total of 83 cells from 15 animals using this type of stimulus.

Several cells with different response properties are depicted in Fig. 3, *A–C*. Generally, cells responded to the onset and offset of light in various degrees. To quantify the response profiles, for each cell we determined the ON response level and the OFF response and calculated the ON/OFF response ratio *R*, which quantifies the ON/OFF polarity of the cell. Cells that exhibit a strong ON response (Fig. 3*A*) will have response ratio close to 1, whereas cells that exhibit a strong OFF response (Fig. 3*B*) will have response ratios close to −1. The response ratio of an ON-OFF cell (Fig. 3*C*) will be close to 0.

We found that most cells respond to both ON and OFF stimulus and that there is a continuum in the response of cells to this kind of stimulus, since the ON/OFF response ratio of different cells spans continuously the interval −1 to 1 (Fig. 3*D*). In addition, there is a slight preference for the OFF stimulus, since the peak of the response histogram is negative (−0.14 ± 0.05, mean ± SE).

Orientation Selectivity in Archer Fish Optic Tectum

The orientation selectivity of cells was tested by flashing a bar on the receptive field center. This was done first by detecting the receptive field boundaries (see MATERIALS AND METHODS) and then by flashing a bar with a matched size in eight different orientations. We recorded 38 cells from 8 animals using this type of stimulus. We quantified the response of different cells to orientation by calculating the orientation index and determined the width of the orientation tuning by fitting a von Mises function only to the cells with high orientation index (for additional details, see MATERIALS AND METHODS).

We found that the response of cells can be classified into two types. The first is a strong response to specific orientation, where the response to the preferred orientation could be up to 20 times higher than the response to the null orientation, and

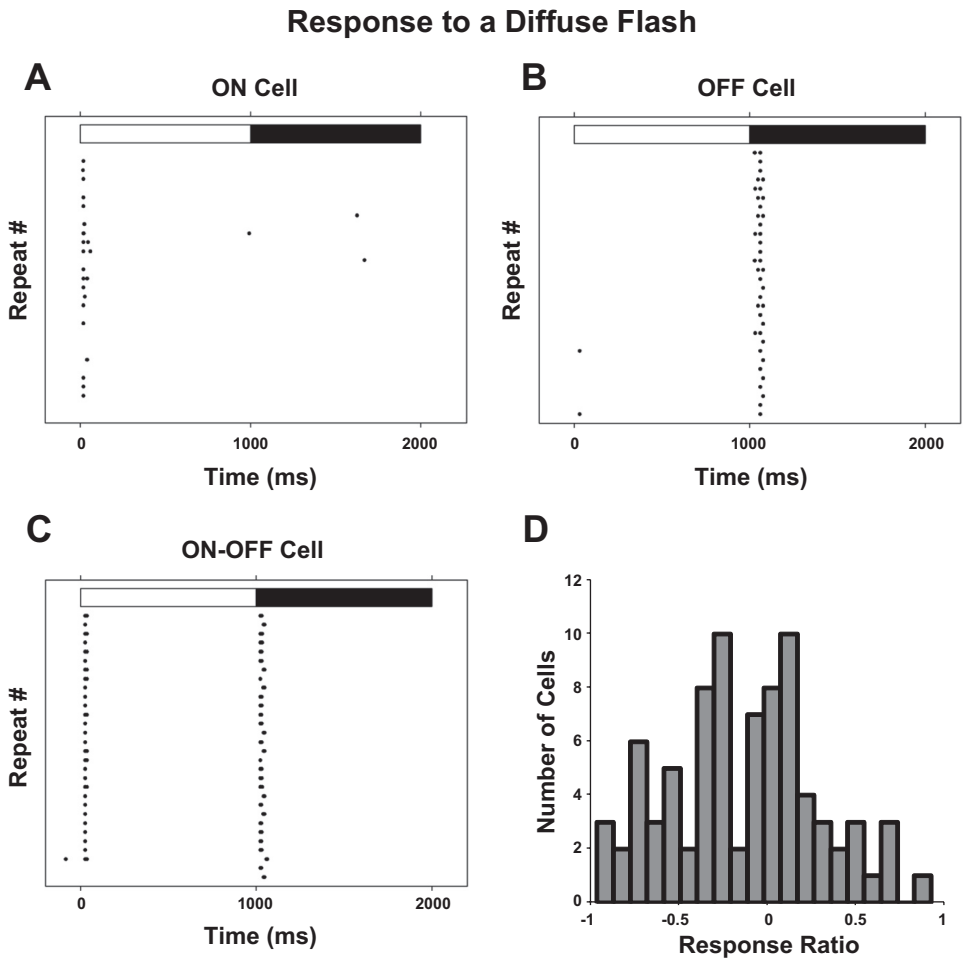

Fig. 3. Cell responses to ON-OFF stimulus. *A*: example of an ON cell, a cell that responds to the onset of a flash. *B*: example of an OFF cell, a cell that responds to the offset of a flash. *C*: example of an ON-OFF cell, a cell that responds to both the onset and offset of a flash. *D*: a distribution of the response ratio of ON and OFF responses shows that the cells fall on a continuum of response patterns between ON and OFF classes. The most abundant pattern is a symmetrical ON-OFF response.

therefore the orientation index is >0.5 (Fig. 4, *A* and *B*). In addition, we found cells with very weak dependence on orientation, where the difference between the maximal and minimal orientation spike count is marginal, for which the orientation index is <0.5 (Fig. 4, *C* and *D*). We define cells with such weak dependence on orientation as orientation-agnostic neurons.

Using this analysis, we found that 58% of the cells were orientation tuned (Fig. 4*E*). We tested the sensitivity of these numbers to the threshold between cell types and found that 10% change in the threshold results with only 1 cell moving between groups. Moreover, the preferred orientation had a strong bias for the vertical orientation with 59% of the orientation-tuned cells having a preference for the vertical orientation or its neighboring orientations (±22.5°), 13.6% of the orientation-tuned cells having a preference for the horizontal orientation or its neighboring orientations (±22.5°), and 27.2% of the orientation-tuned cells having a preference for the other diagonal orientations or its neighboring orientations (±22.5°) (Fig. 4*F*).

We fitted von Mises function to the orientation-tuned cells and explored the parameter κ to find their orientation tuning width. We found that 45% of the cells had a sharp tuning width between 15° and 30°, 41% of the cells had a medium tuning width between 30° and 45°, and 14% of the cells had a tuning width of 45° to 60°. On average, mean orientation tuning width was 33.26° (SE 2.36°; Fig. 4*G*); i.e., the most prevalent width was <34°, indicating that cells in the archer fish optic tectum have relatively sharp orientation tuning profiles.

Direction and Orientation Selectivity of Tectal Neurons in Response to Moving Bars

The direction selectivity of cells in response to moving bars was tested by first locating the receptive field center and then moving a bar across the receptive field (see MATERIALS AND METHODS). We recorded 36 cells from 8 animals using this stimulus. To classify cells into different response groups, we first calculated the spike count in response to specific direction (see MATERIALS AND METHODS) and then calculated the direction index and the orientation index. We then fitted a von Mises function to the response to measure the direction tuning width. For comparison, we also fitted a harmonic function to the response to determine whether our results are robust (see MATERIALS AND METHODS for more details).

We found three types of cells according to their response to a moving bar: *1*) an orientation-tuned response, where the cell responds with high firing rate to movements along a specific axis in space (Fig. 5*A*); *2*) a direction-tuned response, where the cell responds with high rate to movement in a specific direction (Fig. 5*B*); and *3*) an agnostic response, where the cell responds with marginal differences between directions (Fig. 5*C*).

On the basis of the quantitative analysis described above, we found that 11% of the cells were direction tuned, 39% were

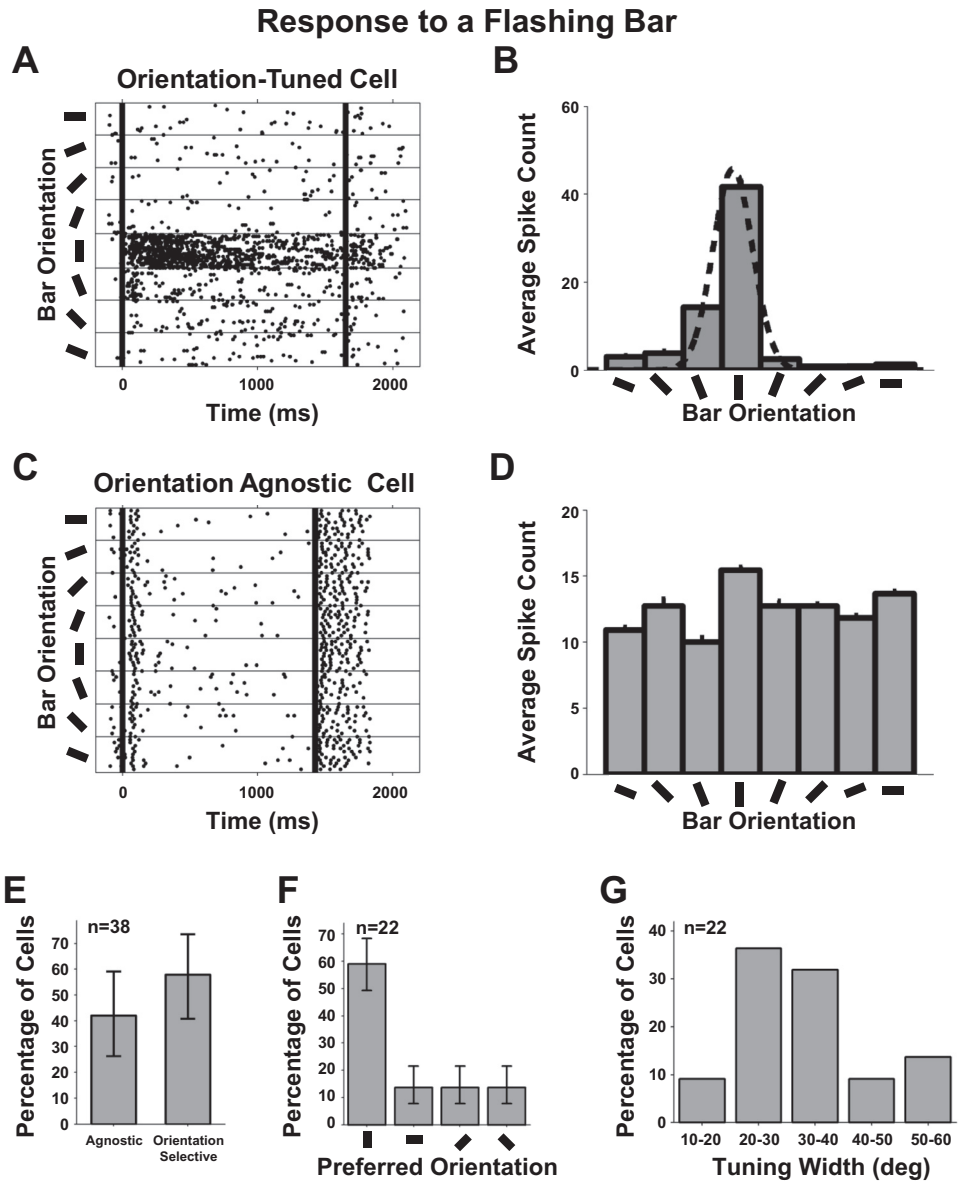

Fig. 4. Orientation selectivity profiles assessed using the static bar stimulus. *A*: raster plots of the responses to the 8 oriented bars for an orientation-tuned cell. Black lines represent the start and end time of the bar display. *B*: orientation tuning profile for the orientation-tuned cell from *A*. The dashed black line represents the fitted von Misses distribution function. *C*: raster plots of the responses to the 8 oriented bars for an orientation-agnostic cell. *D*: orientation tuning profile for the orientation-agnostic cell from *C*. *E*: distribution of selectivity (with 95% confidence interval) for orientation-tuned and orientation-agnostic cells. *F*: distribution of preferred orientation (with 95% confidence interval). The majority of cells preferred the vertical orientation. *G*: distribution of tuning width for the orientation-tuned cells.

orientation tuned, and 50% were classified as direction agnostic (Fig. 5*D*). We tested the sensitivity of these numbers to the threshold between cell types and found that 10% change in the threshold results with 5 cells moving between groups.

Of the orientation-tuned cells, 86% preferred the vertical orientation (as shown in Fig. 5*A*) and 14% preferred the diagonal orientation. We calculated the confidence interval for the possibility of the existence of an additional cell type that we have not observed in our data set (see MATERIALS AND METHODS), orientation-selective cells with a preference for the horizontal orientation. We found that with 95% of certainty, the proportion of this possible missing group is between 0 and 0.1.

We found that half of the direction-tuned cells had the greatest response to a moving bar in the temporal-nasal direction, as determined by exploring the fitted parameter μ in *Eq. 1* and shown in Fig. 5*B*. The other direction-tuned cells preferred the diagonal direction, one from nasal-ventral to caudal-dorsal direction and the other from nasal-dorsal to caudal-ventral direction. The widths of the direction tuning varied between 60° and 90°.

Using the second method, fitting of a harmonic function, to determine the selectivity of the cell in response to a moving bar, we found similar results with a few exceptions. All the cells that were classified as direction-tuned cells with the first method were also classified as direction-tuned cells with the second method. The second method classified an additional cell as a direction-tuned cell. As for the orientation tuning, the second method missed two cells that were classified as orientation-tuned with the first method and added an additional cell as orientation-tuned. Overall, it seems that use of the direction and orientation indexes and the von Mises distribution gives robust results, and moreover, it adds the ability to determine the tuning width, compared with the second method.

Spatial and Temporal Frequency Tuning

The spatial and temporal tuning of cells was evaluated by analyzing the response of cells to sinusoidal grating drifting along the cell's preferred direction. Once the cell preferred direction was detected, we stimulated it with all combinations of six spatial

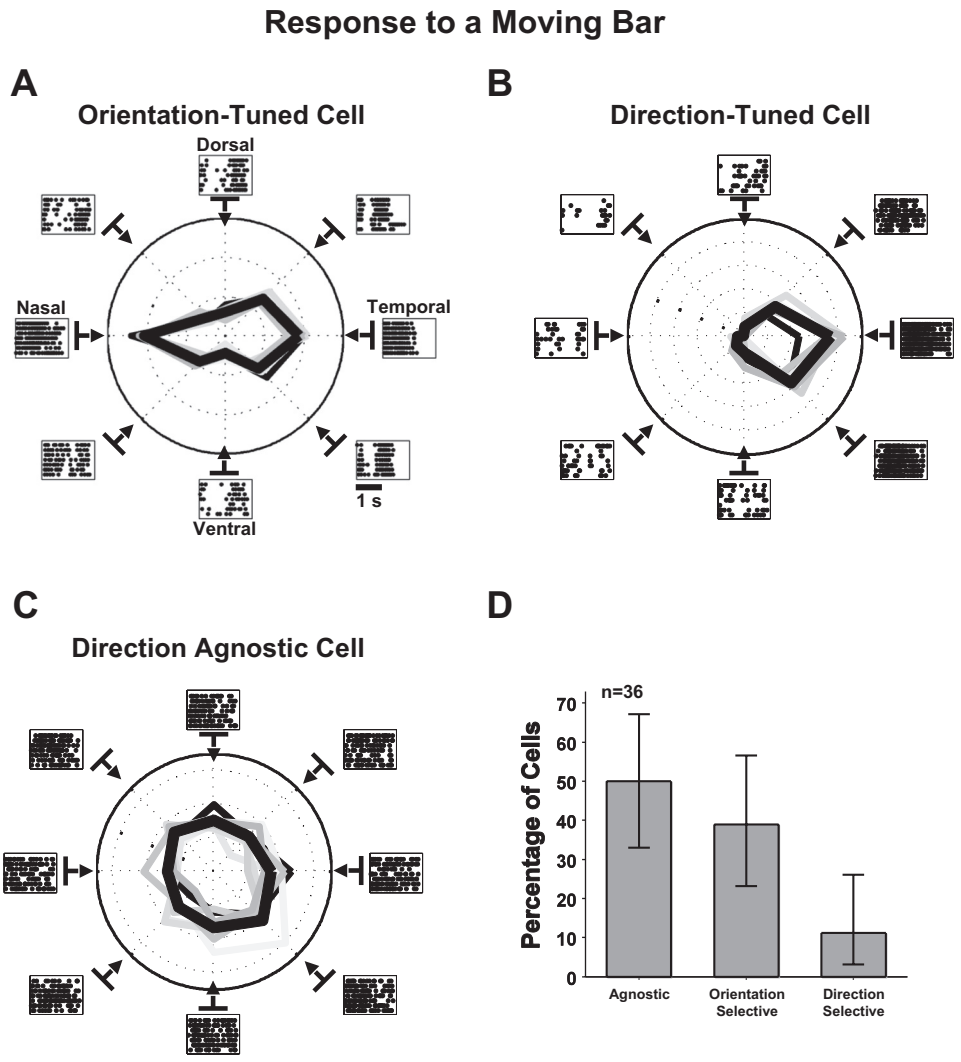

Fig. 5. Direction selectivity profiles assessed using the moving bar stimulus. *A*: orientation-tuned cell profile. *B*: direction-tuned cell profile. *C*: direction-agnostic cell profile. *D*: distribution of selectivity (with 95% confidence interval) for agnostic, orientation-tuned, and direction-tuned cells.

frequencies (ranging from 0.03 to 0.7 cycles/deg) and six temporal frequencies (ranging from 1.5 to 9 Hz). For this stimulus, we recorded a total of 30 cells from 6 animals.

For each cell, we found the combination of spatial and temporal frequencies that elicited the maximal response. The cells had a higher response to a unique combination of spatial and temporal frequencies (Fig. 6, *A* and *B*).

We analyzed the cell response to obtain further frequency tuning properties. To analyze the temporal frequency tuning of a cell, we took the best spatial frequency and analyzed the cellular response for all the different temporal frequencies at that spatial frequency (i.e., 1 row of the response matrix). Fitting a Gaussian function to these responses, we obtained three types of temporal frequency tuning profiles: a low-pass tuning profile, in which cells elicit the maximal response to the lower temporal frequencies tested (Fig. 6*C*); a high-pass tuning profile, in which cells elicit the maximal response to the highest temporal frequencies tested (Fig. 6*D*); and an all-pass tuning profile, in which there was almost no difference in the response to the different temporal frequencies (Fig. 6*E*). We found that 23% of the cells had a low-pass tuning profile, 54% had a high-pass tuning profile, and 23% had an all-pass tuning profile (Fig. 6*H*). We calculated the confidence interval for the possibility of the existence of an additional tuning profile group that we have not observed in our data (see MATERIALS AND METHODS). We found that with 95% of certainty, the proportion of a possible missing group is between 0 and 0.12.

In a similar way, to analyze the spatial tuning of a cell, we took its best temporal frequency and fitted a Gaussian function to the response at all corresponding spatial frequencies (i.e., to 1 column of the response matrix). We found two general types of tuning profiles: low pass and band pass. Figure 6*F* shows a low-pass tuning profile. The maximal response of this cell to the sinusoidal grating is at the lowest spatial frequency tested (0.03 cycles/deg), and at higher spatial frequencies the response gradually decreases. Figure 6*G* shows a band-pass tuning profile. The response of this cell to the sinusoidal grating at the lowest spatial frequency tested (0.03 cycles/deg) and at the highest spatial frequency test (0.7 cycles/deg) is low, and the maximal response is for a spatial frequency in the middle of the range (0.09–0.18 cycles/deg). We found that 57% of the cells had a low-pass tuning profile and 43% of the cells had a band-pass tuning profile (Fig. 6*H*). We calculated the confidence interval for the possibility of the existence of an additional tuning profile group that we have not observed in our data (see MATERIALS AND METHODS). We found that with 95% of certainty, the proportion of a possible missing group is between 0 and 0.12.

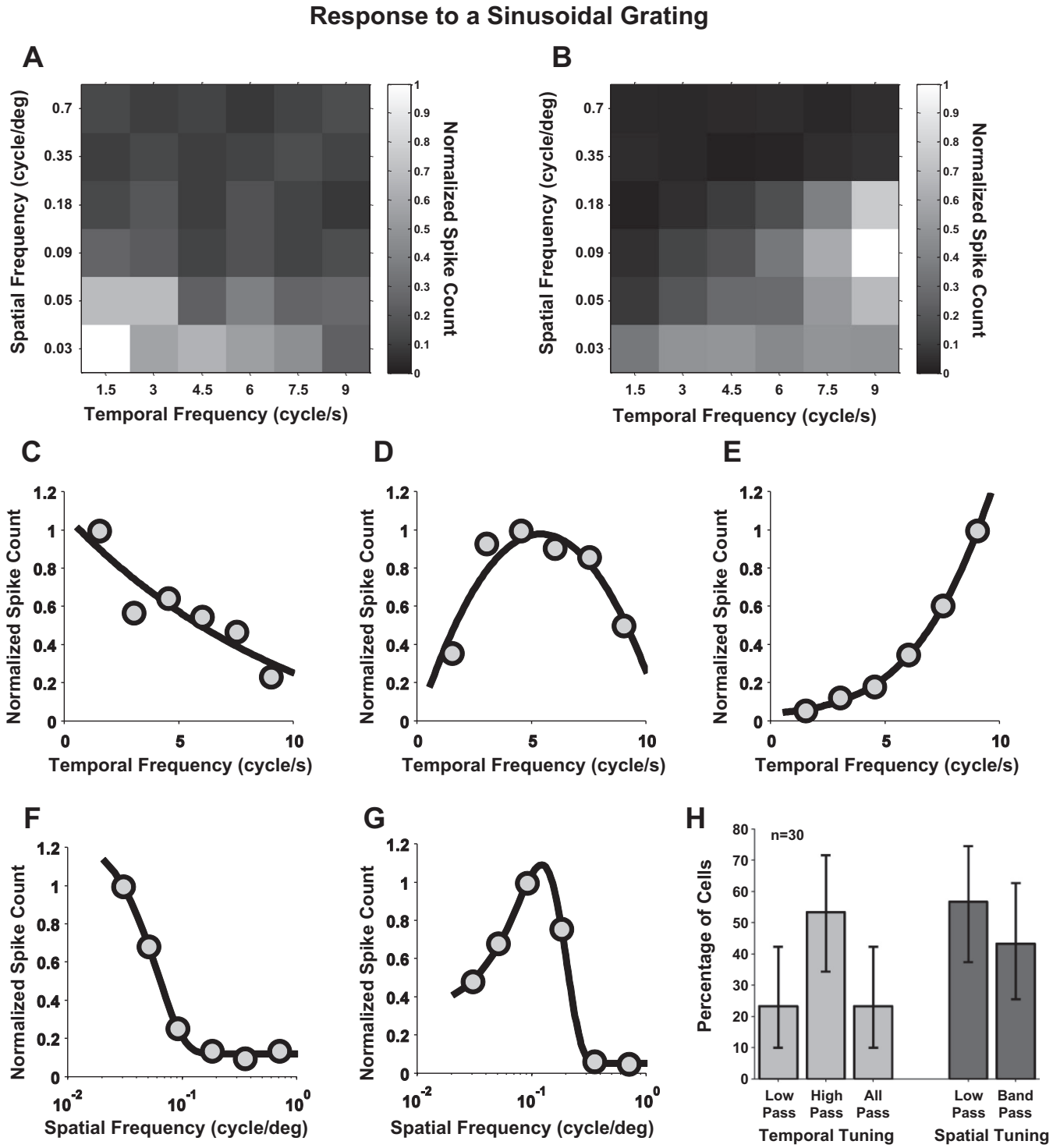

Fig. 6. Responses to spatial and temporal frequencies and tuning profiles assessed using sinusoidal gratings. *A*: example of a cell for which the maximal response rate is at the lowest spatial and temporal frequencies tested. *B*: example of a cell for which the maximal response rate is at one of the central spatial and the highest temporal frequencies tested. *C*: low-pass temporal frequency tuning profile showing the highest response rate at the lowest temporal frequency tested. *D*: high-pass temporal frequency tuning profile showing the highest response rate at the highest temporal frequency tested. *E*: all-pass temporal frequency tuning profile. *F*: low-pass spatial frequency tuning profile showing the highest response rate at the lowest spatial frequency tested. *G*: band-pass spatial frequency tuning profile. *H*: distribution of tuning profiles (with 95% confidence interval). Light gray, temporal frequency tuning; dark gray, spatial frequency tuning. We calculated the confidence interval for the possibility of the existence of an additional tuning profile group that we have not observed in our data (see MATERIALS AND METHODS). For both the spatial frequency and temporal frequency tuning, we found that with 95% of certainty, the proportion of a possible missing group is between 0 and 0.12.

DISCUSSION

Our goal was to explore the visual functional properties of cells in the superficial layers of the optic tectum of the archer fish. We first obtained a retinotectal map of the archer fish optic tectum. We found that the nasal visual field projects to the rostral part of the optic tectum and that the temporal visual field projects to the caudal part of the tectum. In addition, the dorsal visual field projects to the lateral part of the optic tectum, and the ventral visual field projects to the medial part of the optic tectum.

Using a stationary bar stimulus, we found that about 58% of the cells in the superficial layer of the optic tectum (the primary visual area of the archer fish) are orientation tuned. These cells strongly respond to a bar with a specific orientation and are inhibited by a bar of perpendicular orientation. Furthermore, by employing moving bar stimuli, we found that a small fraction (11%) of cells in the optic tectal population is direction tuned. This implies that most cells in the archer fish optic tectum are direction agnostic, unlike the much smaller proportion of such cells in the archer fish ganglion retinal layer (58%; see Tsvilling et al. 2012).

Finally, we studied the response of optic tectal cells to spatial and temporal frequencies using drifting sinusoidal gratings. We found that cells we recorded fall into two major filter categories in their spatial filtering properties: low pass and band pass. Similarly, we found three major types of temporal filtering properties: low pass, all pass, and high pass.

The stimulus used in this study was presented outside the water. Although both the water and the water tank glass are transparent, we should note that there is still a possibility that the fish brain responds in a slightly different manner to stimuli presented within the water body and outside of it. The transformation of receptive field properties in the different environments is interesting for future studies.

Comparison to Optic Tectum of Other Fish

The relation between the visual field and its projection to the contralateral optic tectum has been investigated in four other species of fish (Schwassmann and Kruger 1965). The optic tectum of the archer fish is similar to that of other fish in that the nasal visual field lies on the anterior part of the optic tectum and the temporal visual field lies on its posterior part. Along the dorsal-ventral axis, however, we found that the projection of the dorsal-ventral visual field on the optic tectum is reversed in the archer fish. In all other fish species tested, the dorsal visual field maps to the medial optic tectum (and ventral to lateral), whereas in the archer fish the opposite is the case. A possible explanation for this difference is that as opposed to the other fish mentioned above, the archer fish has a semiterrestrial visual environment, and that property may result in a slightly different retinotectal mapping.

Several studies have tested the functional properties of cells in the optic tectum of the goldfish (Damjanović et al. 2009a, 2009b; Jacobson and Gaze 1964; Maximov et al. 2005). In their study, Maximov et al. (2005) explored the responses of cells to a moving bar stimulus. Using the harmonic function fit, they assigned the cells into three groups, nonselective, orientation-selective and direction-selective cells, using the harmonic function fit, and their study focused on the latter group. Their results reveal that the preferred direction of motion for the majority of the direction-selective cells was the caudal-rostral direction, which is similar to the preferred direction we found in the archer fish direction-tuned cells.

Comparing Early Visual Processing in Archer Fish and Mammals

To put our study in a broad perspective within vision research, we also discuss here the similarities and differences between our findings in the archer fish and the best studies of vertebrates: the mammalian visual system. This comparison can be done on the basis of two different perspectives, evolutionary and functional. The first perspective is based on the observation that the mammalian evolutionary and developmental counterpart of the fish optic tectum is the superior colliculus (Butler and Hodos 2005). The second perspective is based on the fact that the optic tectum in the archer fish is the main region in the fish brain that is devoted to early visual processing (Butler and Hodos 2005), and as such the functional analog for comparison is the mammalian primary visual cortex.

Similarity and Differences Between the Archer Fish Optic Tectum and the Mammalian Superior Colliculus

On the basis of their evolutionary relationship, an obvious question is whether cells with similar functionalities to those we found in the optic tectum of the archer fish exist in the mammalian superior colliculus. Of special interest for this comparison is our finding that part of the cell population in the superficial layer of the optic tectum of the archer fish is direction tuned. Indeed, direction-tuned cells were found in the superior colliculus of the rat (Prévost et al. 2007), the mouse (Wang et al. 2010), and the cat (Pinter and Harris 1981). However, the ratio of direction-tuned cells in the population recorded in our study (11%) is smaller than those observed in the superior colliculus of the mammals (14, 30, and 81% for the rat, mouse, and cat, respectively). The directional tuning widths in the archer fish optic tectum ranged from 60° to 90°, which is higher than the directional tuning widths of cells in the superior colliculus of the mouse (40.9 $\pm$ 1.3°) and smaller than those of the rat (146.7 $\pm$ 89.2°).

Unlike those in mammals, where preferred direction tends to have a horizontal component (Prévost et al. 2007) or both a vertical and horizontal component (Berman and Cynader 1972), archer fish optic tectum cells have bias toward the vertical direction. A possible explanation for this difference is the different visual environment in which the fish and mammals live. Mammals usually live in an environment where the horizon is a very salient feature in the visual field, whereas the archer fish live in water that is a three-dimensional world with a preference to look above water for insects as a possible food source and birds as possible predators. Naturally, whether or not the natural environment plays a critical role in the direction selectivity of the species may be confirmed with marine mammals.

The other salient property we found in the archer fish optic tectum is orientation selectivity. Orientation-tuned cells were also found in the superior colliculus of the mouse (Wang et al. 2010) and the rat (Prévost et al. 2007), but not in that of the cat or the monkey. Again, the preferred orientation of the cells in these two mammals is biased toward the horizontal orientation, whereas in the archer fish it is biased toward the vertical orientation.

Studies have tested the temporal tuning properties of the cells in the superior colliculus of rodents. It was found that only 20% of cells in the rat superior colliculus (Prévost et al. 2007) showed a high-pass tuning profile, and the majority of the cells preferred lower temporal frequencies, with a mean of 3.5 Hz. In the mouse, 97% of the superior colliculus cells that were tested preferred temporal frequencies between 0.5 and 4 Hz (Wang et al. 2010). This is in contrast to our findings, where 54% of the cells preferred high temporal frequency, e.g., temporal frequency higher than 8 Hz.

As for the spatial frequency tuning profile, there is similarity between the optic tectum cells of the archer fish and the superior colliculus cells of the rat (Prévost et al. 2007) and the mouse (Wang et al. 2010). We found that the preferred spatial frequency of cells is in the range of 0.03–0.18 cycles/deg. In the superior colliculus of the mouse, almost all the cells had preferred spatial frequencies between 0.02 and 0.16 cycles/deg. In the rat, the range of preferred spatial frequency was 0.01–0.1 cycles/deg, which is slightly lower than the preferred spatial frequencies in the archer fish optic tectum cells.

To conclude, we found many similarities between the functional units in the archer fish optic tectum and the mammalian superior colliculus. However, one should keep in mind that these two structures exist in two very different animals that represent large evolutionary distance and many differences in habitat.

Similarity and Differences Between the Archer Fish Optic Tectum and the Mammalian Visual Cortex

Considered functionally, the mammalian brain structure analogous to the fish optic tectum is the visual cortex, since both are the primary visual areas of their respective species. Since Hubel and Wiesel (1959) discovered the orientation and direction selectivity properties in the cat striate cortex, a great body of research has accumulated exploring these types of cells in the mammalian cortex (Albright 1984; Blasdel and Fitzpatrick 1984; Bradley et al. 1987; De Valois et al. 1982; Gizzi et al. 1990; Hawken and Parker 1984; Hubel and Wiesel 1968; Mansfield and Ronner 1978; Rose and Blakemore 1974; Sclar and Freeman 1982; Weliky et al. 1996). Indeed, in this article we report similar tuning properties in the archer fish optic tectum, as well.

At first we examined the orientation selectivity property. We have found that 58% of the cells we recorded were orientation-tuned cells by analyzing their response to a stationary bar flash. Furthermore, we found that 86% of the orientation-tuned cells that responded to the moving bar stimulus and 59% of the orientation-tuned cells in the stationary bar stimulus had a preference for the vertical orientation of the bar. However, in the mammalian cortex the picture is slightly different. It was found that in the cat (Rose and Blakemore 1974) and the monkey (De Valois et al. 1982; Mansfield and Ronner 1978) visual cortex, the vast majority of cells were selective to the orientation of a line stimulus; however, there was no significant preference for a specific orientation, but rather for a wide range of orientations. Nevertheless, a further division of cells to foveal cells vs. parafoveal cells revealed that foveal cells in the cat/monkey/hamster showed higher firing rates in response to vertical and horizontal orientations than to diagonal orientations (De Valois et al. 1982). In addition, we found that the tuning width of orientation-tuned cells in the archer fish optic tectum ranged from 15° to 60° (mean: 33.26 ± 2.36°), which is bigger than tuning widths of the cat's cortical orientation-tuned cells (mean: 18.2 ± 1.1°) and smaller than those of the monkey's (mean: 40.7°).

Examination of direction-tuned cells yields similar conclusions. The fraction of direction-tuned cells in the archer fish superficial layer of the optic tectum (11%) is much smaller than that of the direction-tuned units found in the cat and monkey visual cortex [64, 83 and 89% in the cat striate cortex, cat suprasylvian cortex, and monkey V1, respectively (Albright 1984; Gizzi et al. 1990)]. Again, no clear bias toward a specific preferred direction of motion in the mammalian cortex was seen, in contrary to the bias toward the temporal-nasal movement direction that we found in the archer fish.

Functional Implications of This Study

We found that cells in the superficial layers of the archer fish optic tectum have diverse functional properties. By comparing the archer fish optic tectum with its functionally equivalent area in mammals, the visual cortex, we were able to find similarities and differences between the functional properties of neurons in these regions. The current agreement is that the response of V1 consists of neurons with a variety of selective spatiotemporal filters. These filters are believed to be well suited to the statistics of natural images (Field 1987; Olshausen and Field 1996). We showed here that the optic tectum cells also can be considered as spatiotemporal filters. One may ask whether these filters are suited to the statistics of the aquatic natural images.

It was suggested that there is a connection between the functional properties of cells in the visual cortex and the performance in specific visual tasks such as visual search and orientation and motion discrimination (Kastner et al. 1999; Knierim and Van Essen 1992). This ability is due to the cell selectivity for basic visual features such as orientation and motion selectivity. It will be interesting to explore whether the archer fish can perform visual tasks in a similar way and whether a similar connection between the behavioral level and the functional properties of cells exists.

ACKNOWLEDGMENTS

We thank G. Glusman for technical assistance.

GRANTS

This research was supported by The Israel Science Foundation Grant 207/11.

DISCLOSURES

No conflicts of interest, financial or otherwise, are declared by the authors.

AUTHOR CONTRIBUTIONS

M.B.T., I.K., and C.G. performed experiments; M.B.T., O.D., O.B.S., and R.S. analyzed data; M.B.T., O.D., O.B.S., and R.S. interpreted results of experiments; M.B.T. prepared figures; M.B.T. and R.S. drafted manuscript; M.B.T., O.D., O.B.S., and R.S. edited and revised manuscript; M.B.T., C.G., and R.S. approved final version of manuscript; R.S. conception and design of research.

REFERENCES

Albright TD. Direction and orientation selectivity of neurons in visual area MT of the macaque. *J Neurophysiol* 52: 1106–1130, 1984.

Baron J, Pinto L, Dias MO, Lima B, Neuenschwander S. Directional responses of visual wulst neurones to grating and plaid patterns in the awake owl. *Eur J Neurosci* 26: 1950–1968, 2007.

Bastian J. Vision and electroreception: integration of sensory information in the optic tectum of the weakly electric fish *Apteronotus albifrons*. *J Comp Physiol* 147: 287–297, 1982.

Ben-Simon A, Ben-Shahar O, Segev R. Measuring and tracking eye movements of a behaving archer fish by real-time stereo vision. *J Neurosci Methods* 184: 235–243, 2009.

Ben-Simon A, Ben-Shahar O, Vasserman G, Ben-Tov M, Segev R. Visual acuity in the archerfish: behavior, anatomy, and neurophysiology. *J Vis* 12: 18, 2012a.

Ben-Simon A, Ben-Shahar O, Vasserman G, Segev R. Predictive saccade in the absence of smooth pursuit: interception of moving targets in the archer fish. *J Exp Biol* 215: 4248–4254, 2012b.

Berman N, Cynader M. Comparison of receptive-field organization of the superior colliculus in Siamese and normal cats. *J Physiol* 224: 363–389, 1972.

Blasdel GG, Fitzpatrick D. Physiological organization of layer 4 in macaque striate cortex. *J Neurosci* 4: 880–895, 1984.

Bodznick D. Elasmobranch vision: multimodal integration in the brain. *J Exp Zool* 256, *Suppl* 5: 108–116, 1990.

Bradley A, Skottun BC, Ohzawa I, Sclar G, Freeman RD. Visual orientation and spatial frequency discrimination: a comparison of single neurons and behavior. *J Neurophysiol* 57: 755–772, 1987.

Butler AB, Hodos W. *Comparative Vertebrate Neuroanatomy: Evolution and Adaptation*. New York: Wiley-Liss, 2005.

Catania K, Leitch D, Gauthier D. Function of the appendages in tentacled snakes (*Erpeton tentaculatus*). *J Exp Biol* 213: 359–367, 2010.

Damjanović I, Maximova E, Maximov V. On the organization of receptive fields of orientation-selective units recorded in the fish tectum. *J Integr Neurosci* 8: 323–344, 2009a.

Damjanović I, Maximova E, Maximov V. Receptive field sizes of direction-selective units in the fish tectum. *J Integr Neurosci* 8: 77–93, 2009b.

De Valois RL, Yund EW, Hepler N. The orientation and direction selectivity of cells in macaque visual cortex. *Vision Res* 22: 531–544, 1982.

Field DJ. Relations between the statistics of natural images and the response properties of cortical cells. *J Opt Soc Am A* 4: 2379–2394, 1987.

Fisher NI. *Statistical Analysis of Circular Data*. Cambridge, UK: Cambridge University Press, 1995.

Gizzi MS, Katz E, Schumer RA, Movshon JA. Selectivity for orientation and direction of motion of single neurons in cat striate and extrastriate visual cortex. *J Neurophysiol* 63: 1529–1543, 1990.

Hawken M, Parker A. Contrast sensitivity and orientation selectivity in lamina IV of the striate cortex of Old World monkeys. *Exp Brain Res* 54: 367–372, 1984.

Hubel DH, Wiesel TN. Receptive fields and functional architecture of monkey striate cortex. *J Physiol* 195: 215–243, 1968.

Hubel DH, Wiesel TN. Receptive fields of single neurones in the cat's striate cortex. *J Physiol* 148: 574–591, 1959.

Jacobson M, Gaze R. Types of visual response from single units in the optic tectum and optic nerve of the goldfish. *Exp Physiol* 49: 199–209, 1964.

Kastner S, Nothdurft H, Pigarev IN. Neuronal responses to orientation and motion contrast in cat striate cortex. *Vis Neurosci* 16: 587–600, 1999.

Kinoshita M, Ito E. Roles of periventricular neurons in retinotectal transmission in the optic tectum. *Prog Neurobiol* 79: 112–121, 2006.

Kinoshita M, Ueda R, Kojima S, Sato K, Watanabe M, Urano A, Ito E. Multiple-site optical recording for characterization of functional synaptic organization of the optic tectum of rainbow trout. *Eur J Neurosci* 16: 868–876, 2002.

Knierim JJ, Van Essen DC. Neuronal responses to static texture patterns in area V1 of the alert macaque monkey. *J Neurophysiol* 67: 961–980, 1992.

Knudsen EI. Auditory and visual maps of space in the optic tectum of the owl. *J Neurosci* 2: 1177–1194, 1982.

Mansfield RJ, Ronner SF. Orientation anisotropy in monkey visual cortex. *Brain Res* 149: 229–234, 1978.

Maximov V, Maximova E, Maximov P. Direction selectivity in the goldfish tectum revisited. *Ann NY Acad Sci* 1048: 198–205, 2005.

Mokeichev A, Segev R, Ben-Shahar O. Orientation saliency without visual cortex and target selection in archer fish. *Proc Natl Acad Sci USA* 107: 16726–16731, 2010.

Nevin LM, Robles E, Baier H, Scott EK. Focusing on optic tectum circuitry through the lens of genetics. *BMC Biol* 8: 126, 2010.

Olshausen BA, Field DJ. Natural image statistics and efficient coding. *Network* 7: 333–339, 1996.

Pinter RB, Harris LR. Temporal and spatial response characteristics of the cat superior colliculus. *Brain Res* 207: 73–94, 1981.

Prévost F, Lepore F, Guillemot JP. Spatio-temporal receptive field properties of cells in the rat superior colliculus. *Brain Res* 1142: 80–91, 2007.

Rose D, Blakemore C. An analysis of orientation selectivity in the cat's visual cortex. *Exp Brain Res* 20: 1–17, 1974.

Sajovic P, Levinthal C. Visual cells of zebrafish optic tectum: mapping with small spots. *Neuroscience* 7: 2407–2426, 1982.

Schlegel T, Schuster S. Small circuits for large tasks: high-speed decision-making in archerfish. *Science* 319: 104–106, 2008.

Schuster S. Fast-starts in hunting fish: decision-making in small networks of identified neurons. *Curr Opin Neurobiol* 22: 279–284, 2012.

Schuster S, Wöhl S, Griebsch M, Klostermeier I. Animal cognition: how archer fish learn to down rapidly moving targets. *Curr Biol* 16: 378–383, 2006.

Schwassmann HO, Kruger L. Organization of the visual projection upon the optic tectum of some freshwater fish. *J Comp Neurol* 124: 113–126, 1965.

Sclar G, Freeman R. Orientation selectivity in the cat's striate cortex is invariant with stimulus contrast. *Exp Brain Res* 46: 457–461, 1982.

Temple S, Manietta D, Collin S. A comparison of behavioural (Landolt C) and anatomical estimates of visual acuity in archerfish (*Toxotes chatareus*). *Vision Res* 83: 1–8, 2013.

Temple S, Hart NS, Marshall NJ, Collin SP. A spitting image: specializations in archerfish eyes for vision at the interface between air and water. *Proc Biol Sci* 277: 2607–2615, 2010.

Timmermans P. Prey catching in the archer fish: marksmanship, and endurance of squirting at an aerial target. *Neth J Zool* 50: 411–423, 2000.

Timmermans P. Prey catching in the archer fish: angles and probability of hitting an aerial target. *Behav Processes* 55: 93–105, 2001.

Tsvilling V, Donchin O, Shamir M, Segev R. Archer fish fast hunting maneuver may be guided by directionally selective retinal ganglion cells. *Eur J Neurosci* 35: 436–444, 2012.

Vanegas H, Ito H. Morphological aspects of the teleostean visual system: a review. *Brain Res Rev* 6: 117–137, 1983.

Vasserman G, Shamir M, Ben Simon A, Segev R. Coding "what" and "when" in the archer fish retina. *PLoS Comput Biol* 6: e1000977, 2010.

Wang L, Sarnaik R, Rangarajan K, Liu X, Cang J. Visual receptive field properties of neurons in the superficial superior colliculus of the mouse. *J Neurosci* 30: 16573–16584, 2010.

Weliky M, Bosking W, Fitzpatrick D. A systematic map of direction preference in primary visual cortex. *Nature* 379: 725–728, 1996.